Volume 3, Issue 1 (2015) 284-289 ISSN 2347 - 3258
International Journal of Advance Research and Innovation

Soft Switching of Phase Shifted Full Bridge DC-DC Converter

Suthirganesh. H [a], Kalyanasundaram [b]
[a] Department of Electrical and Electronics Engineering, Vandayar Engineering College, Thanjavur, Tamil Nadu, India
[b] Department of Dairy Engineering, SMC College of Dairy Science, Anand Agricultural University, India

Article Info
Article history:
Received 10 February 2015
Received in revised form
15 February 2015
Accepted 28 February 2015
Available online 15 March 2015

Keywords
Isolated dc-dc microconverter, photovoltaic (PV)

Abstract
Effective photovoltaic power conditioning requiresufficient power conversion and accurate maximum power pointtracking to counteract the effects of panel mismatch, shading, andgeneral variance in power output during a daily cycle. In this paper,the authors propose anboost converter withlow component count, galvanic isolation, simple control, as well ashigh efficiency across a wide input and load range. Provided is adiscussion of the converter synthesis, key operational features, converterdesign procedure, and loss analysis, as well as experimentalverification by way of a 250-W prototype with a California EnergyCommission efficiency of 96.8%.

1. Introduction

POWER conversion for photovoltaic (PV) applications, as opposed to more conventional dc–dc converter configurations, requires an adaptable system that is capable of responding to a wide range of input voltage and current conditions. As previously stated in the literature, PV voltage varies significantly with panel construction and operating temperature, while the PV current changes largely due to solar irradiance and shading conditions [1]. If a converter is designed only for high peak efficiency, oftentimes the range of conditions common to many PV installations will force the converter into another operating region where it is much less efficient. Thus, the California Energy Commission (CEC) has introduced a more comprehensive scale for measuring converter performance, a so-called weighted efficiency, as an attempt to reflect the net efficiency of a power conditioning system (PCS) over the course of an average day [2], [3].

Also of interest in the PV PCS design process is the necessity of galvanic isolation between the PV panel and the electric utility system. While an ungrounded, grid-connected PV arrayis permitted by many electric codes, galvanic isolation can be preferred for various reasons. Most notable among these are improved voltage boost ratio, reduced ground leakage current, and overall safety improvement during fault conditions [4]–[6].

Existing Diagram

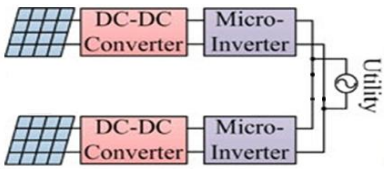

Proposed Diagram

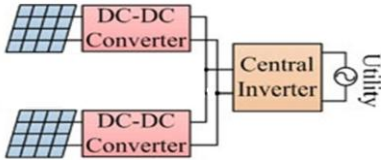

Corresponding Author,
E-mail address:

As several authors have already proposed, distributed maximum power point tracking (MPPT) can achieve much better energy harvesting over systems that are completely centralized[7]. Researchers have also concluded that a system structure with the PV panels connected in parallel can be much more productive in low-light and partially shaded conditions than a series-connected system [8]–[12]. These concerns arguably make the single-panel PV micro inverter (dc–ac), or at least an isolated micro converter (dc–dc), an attractive option from a strictly performance-based analysis. In either system, the dc–dc stage implements local MPPT optimization, while the second stage attempts to regulate the dc-link voltage by sending power to the utility grid. Block diagrams showing the micro inverter and micro converter system structures are provided in Fig. 1. It is this combination of high CEC efficiency, galvanic isolation, and a localized, distributed approach to energy conversion that has prompted the proceeding technical development.

In the literature, there have been a variety of different methods proposed for micro conversion, both isolated and no isolated [13]–[16]. Some utilize one pulse width-modulated (PWM) stage in the conversion from dc–ac [17], others utilize multiple PWM stages. For reasons discussed earlier, the authors are constraining the discussion henceforth to isolated solutions. Considering also only multistage solutions allows for increased interoperability between distributed ac and dc systems while permitting the removal of electrolytic capacitors, which have limited lifetime, from the system design.

In the distributed PV PCS, the isolated dc–dc stage must operate efficiently at full power, while maintaining high performance at light load, across a range of PV voltages. In order to maintain high efficiency under low-power conditions, it is necessary to minimize the amount of circulating energy in the system. An alternate definition of this characteristic would be producing a system with a high "power factor" at the isolation transformer. Also critical to light load efficiency is mitigating the devices witching loss. Finally, reduction of the control and gate drive complexity allows for lower fixed losses due to auxiliary power requirements. When considering potential PV conversion solutions, addressing these loss mechanisms is critical to a successful design.

One popular option for the dc–dc conversion stage is a simple continuous-conduction-mode (CCM) fly back converter [18], [19]. It has the benefit of simple construction and low circulating energy. However, the switching loss for both the primary switch and the diode can be quite large, and the overall system efficiency is typically low (<90%). Improvements in fly back efficiency can be made using variants such as zero-voltage transition or active clamp, both of which use the transformer leakage inductance as a resonant element to achieve zero-voltage switching (ZVS) across the main device [20], [21]. However, this effectively trades switching loss for circulating energy, reducing efficiency at high line or low power. Another more complex effort involves transitioning between different circuit topologies at different load/line conditions thereby increasing control and system complexity [22].

Another option is the series-resonant converter, and more recently the LLC resonant converter, both of which operate on a similar principle and, typically, use a variable frequency control to adjust the output voltage [23]–[25].When the series-resonant, or LLC converter, is operated near the resonant frequency of the tank circuit, the converter achieves nearly ZVS and zero-current switching (ZCS) with very low circulating energy, giving it a high peak efficiency. However, as the operating frequency diverges from the resonant frequency, the amount of circulating energy increases. Unfortunately, the normal conditions for PV conversion will often push the converter significantly away from the optimum switching frequency, causing the CEC efficiency to suffer. Several authors have proposed methods to extend the line and load range of the LLC, once again complicating the circuit topology and control [26]–[28]. Other authors have proposed using the series-resonant converter as an unregulated dc–dc transformer (DCX) [29]. This approach has the benefit of almost no switching loss, little or no circulating energy, very high peak efficiency, and integrated isolation. However, the inverter stage must be able to regulate over a wide input range because the PV voltage fluctuates so dramatically, causing extremely poor overall system efficiency.

This concept of using the series-resonant DCX is not without merit, but the system requires an additional element to provide regulation capability. The method proposed in this paper integrates a traditional boost converter element into the DCX with only the addition of a single inductor. The overall design is straightforward and may be controlled using simple fixed frequency PWM with only the need to observe limitations on the maximum and minimum duty cycle. For PV applications, this circuit satisfies the need for galvanic isolation, low switching loss (the output diodes achieve ZCS), minimal circulating energy, as well as simple gate drive and control. In the following sections, the authors will discuss the synthesis of the topology, key waveforms and operational characteristics, design procedure and loss analysis, as well as experimental results for a250-W prototype.

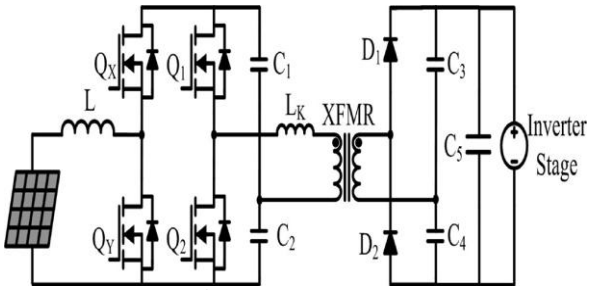

Fig: 2. Resonant half-bridge with separate boost input stage.

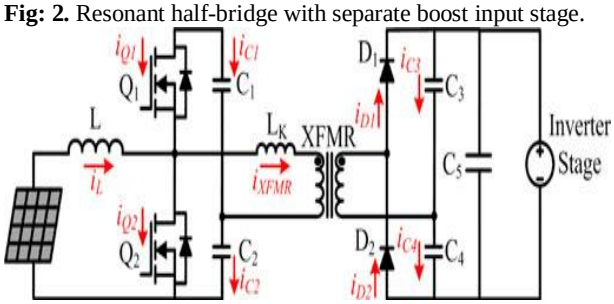

Fig: 3. IBR Converter

2. Converter Synthesis and Operation

When considering the series-resonant DCX as part of this new hybrid circuit, it is important to notice the half-wave resonant behavior by which it operates. During the on-period of either switch a resonant circuit is formed by a combination of the input-side capacitors, the output-side capacitors, and the transformer leakage inductance. The unidirectional nature of the output diodes prevents this circuit from resonating perpetually, and instead, only a resonant period consisting of one half-sine wave is visible. Provided that this resonant period is allowed to complete fully before the primary-side switches change states, the series-resonant circuit is naturally soft-switching on both turn-on and turn-off (ZVS and ZCS). If both resonant periods are allowed to fully complete, the system has no method by which to regulate the output, and the output is simply a reflection of the input. Hence, the necessary addition of another "regulating element," in this case a boost converter, is shown in Fig.2. The boost converter regulates the effective input voltage to the series-resonant converter, allowing it to run as a DCX with high efficiency. The cost is two additional transistors, with their associated gate drive requirements, and some additional switching and conduction loss.

This circuit may be further simplified by integrating the system so that the boost converter function is implemented by the original two MOSFETs. A straightforward method to understand this is to directly tie the input inductor to the midpoints of both active switching legs simultaneously. Note that this change directly ties the inductor to one terminal of the transformer. This additional connection renders the upper MOSFETs (*QX*and*Q*1) as well as the lower MOSFETs (*QY* and*Q*2) in parallel, so long as their switching patterns are synchronized. Thus, the circuit may be simplified, with the additional connection and the removal of *QX* and *QY*, into the topology shown in Fig. 3.Because the now single upper and lower FETs (*Q*1 and *Q*2)are effectively replacing two parallel FETs, they carry the combined current from the original four switches. Also,

as long as the resonant behavior is allowed to complete, the output diodes, *D*1 and *D*2 , still achieve ZCS.

Mode 1:

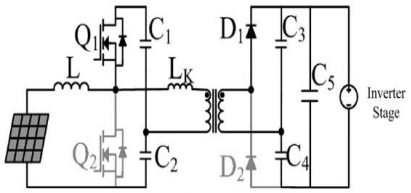

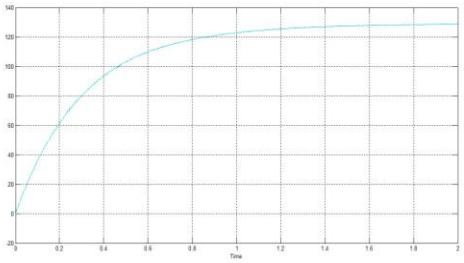

Mode 1 Operation

- *[t*0 < *t* < *t*1*]*
- Beginning with the turnoff of *Q*2 prior to *t*0 , the current in the input inductor *L* flows into the body diode of *Q*1 , discharging its parasitic capacitance.
- This allows *Q*1 to be turned ON under ZVS conditions at *t*0. At this time, the upper input-side capacitor *C*1 begins resonating with the transformer leakage inductance *Lk*and the output-side capacitors, *C*3 and *C*4 , through *D*1 .
- Simultaneously, the input current begins charging the series combination of *C*1 and *C*2 .
- During this phase, *Q*1 carries the difference between the transformer current, flowing from *C*1 through the positive terminal of the transformer and the input current.
- Once the transformer current resonates back to zero, *D*1 prevents the continued resonating in the reverse direction, ending mode 1.

The length of mode 1 is given by

$$T_{res1} = \pi\sqrt{L_k\left[\frac{n^2(C_1+C_2)(C_3+C_4)}{C_1+C_2+n^2(C_3+C_4)}\right]}.$$

- Lk-leakage inductance
- C1-upper input-side capacitor
- C2-lower input-side capacitor
- C3, C4-output-side capacitor

Mode 2:

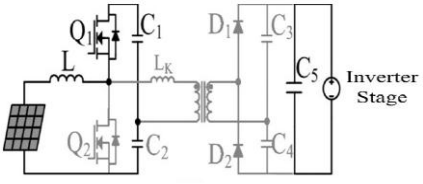

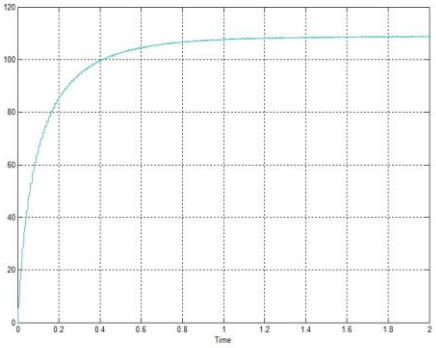

Mode 2 Operation:

- [t1 < t < t2]
- Q1 is still active, yet it is only conducting the input inductor current, which is still decreasing, a pathway which is shown in Fig. The resonant elements all conduct zero current during this interval. Only C5 continues discharging into the load at this time.
- Mode 2 ends with the turn-off of Q1 and the subsequent turn-on of Q2.

Mode 3

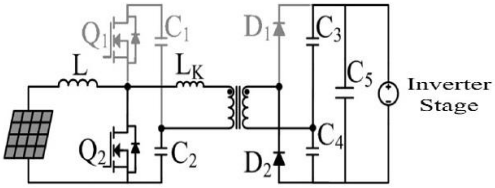

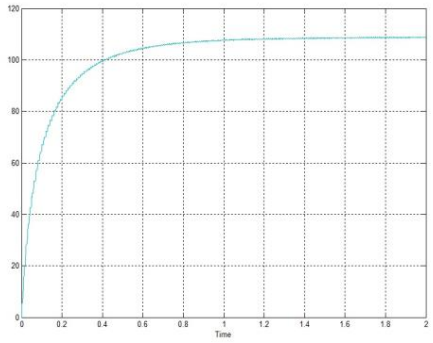

Mode 3 Operation

- [t2 < t < t3]
- After the turn-off of Q1, but prior the turn-on of Q2, the inductor current is still shunted into charging the series combination of C1 and C2, this time through the body diode of Q1 , and still decreasing almost linearly. When Q2 is turned ON, the body diode of Q1 is hard commutated, causing some switching loss.
- At t2, C2 begins to resonate with Lkand the parallel combination of C3 and C4 , through the diode D2 . Simultaneously, the inductor current also flows through Q2, increasing linearly. During this interval, Q2 carries the sum of the transformer current and the inductor current.
- Thus, the rms current through Q2 is significantly larger than that of Q1, which carries the difference of the two

currents. Once the transformer current resonates back to zero, D2 blocks the continued oscillation, marking the end of mode 3

Mode 4

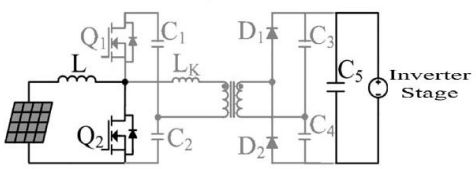

$$T_{res2} = \pi\sqrt{\frac{L_k C_2 n^2 (C_3 + C_4)}{C_2 + n^2 (C_3 + C_4)}}.$$

Mode 4 Operation:

- [t2 < t < t3]
- After the turn-off of Q1, but prior the turn-on of Q2, the inductor current is still shunted into charging the series combination of C1 and C2, this time through the body diode of Q1 , and still decreasing almost linearly. When Q2 is turned ON, the body diode of Q1 is hard commutated, causing some switching loss.
- At t2, C2 begins to resonate with Lkand the parallel combination of C3 and C4 , through the diode D2 . Simultaneously, the inductor current also flows through Q2, increasing linearly. During this interval, Q2 carries the sum of the transformer current and the inductor current.
- Thus, the rms current through Q2 is significantly larger than that of Q1, which carries the difference of the two currents.

Once the transformer current resonates back to zero, D2 blocks the continued oscillation, marking the end of mode 3

3. Experimental Results

During the course of this development, a 250-W prototype converter was designed and built in order to validate the presented analysis and to serve as a core element in a new distributed PV generation system. Some specifications for the circuit are listed in Tables I and II, while the semiconductor device contents summarized in Table III. Table IV includes the switching data for Q1 and Q2 used in the calculations loss analysis above. The system control was implemented digitally on a Texas Instruments TMS320F28026 microcontroller simply for flexibility and rapid implementation. In practice, a dedicated PWM or MPPT controller would also function well. A photograph of the prototype is provided in Fig. 7.

Figs. 8 and 9 demonstrate the consistency of the converter operation over both high and low power. Under each condition, both the inductor current and the transformer current retain their general wave shape while demonstrating CCM and resonant behavior, respectively. This consistency and simplicity is further demonstrated by the voltage transfer ratio plot in Fig. 10, which shows the relationship of the voltage transfer ratio given in (1), as compared to experimental measurement at low and high power.

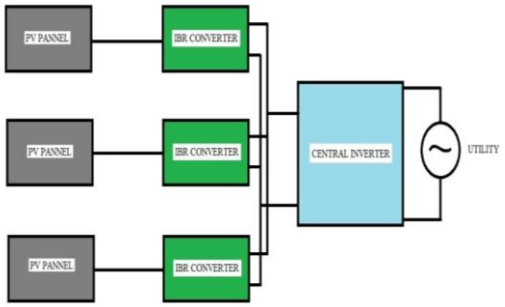

Block Diagram

In order for the converter to achieve high efficiency, two other critical components were mentioned, mitigating switching loss and improving transformer power factor. One definitive aspect of managing the converter switching loss is the ability of the output diodes to achieve ZCS. Experimental evidence of this is provided in Fig. 11, even at high power (>225 W). Also, the fully resonant behavior at the transformer allows the converter to achieve a high power factor, as evidenced in Fig. 12. Here, it is shown that the transformer current is continually in-phase with the transformer voltage, indicating very low circulating energy.

Utilizing the TI microcontroller, a simple PV voltage control loop with P&O MPPT logic was implemented, similar to [38]. At startup, the converter starts at the open-circuit voltage of the PV panel and attempts to locate the MPP by changing the input voltage reference and measuring the corresponding change in input power. An experimental waveform showing the proposed IBR converter operation during startup (via connecting the converter to the PV panel), MPPT operation, as well as shutdown (via forcibly disconnecting the PV panel from the input) is shown in Fig. 13. For the test recorded in the figure, a BP Solar SX6165N polycrystalline SiN PV panel was used as the input source, which has characteristics recorded in Table.

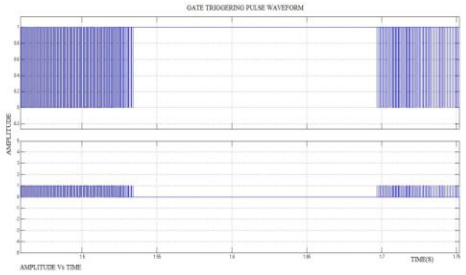

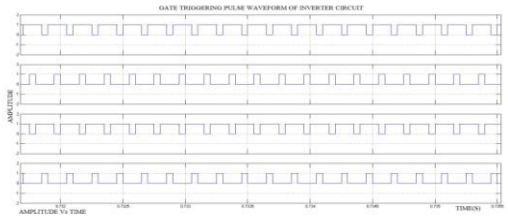

As the final step in the verification process, an experiment to demonstrate the efficiency of the proposed converter was conducted. Projections for the converter efficiency, based on the procedure outlined in Section III,

are given in Fig. 14. Shown in Fig. 15 is the measured power stage efficiency for a range of input and load conditions. These match well overall, with some discrepancies at full power due to un modeled circuit parasitic. Another issue is the variation in the device switching times under different current conditions, causing a low estimate of the efficiency at the low-voltage conditions. However, the converter achieves a CEC efficiency of 96.8% and an overall peak efficiency of 97.4%.

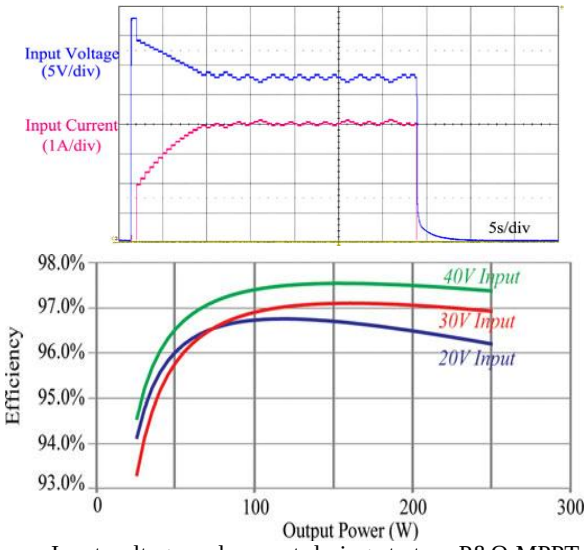

Input voltage and current during startup, P&O MPPT, and shutdown using a BP Solar SX6165N 165-W PV Panel (112-W operating power) (400-Vdc output).Projected power stage efficiency (400-Vdc output)

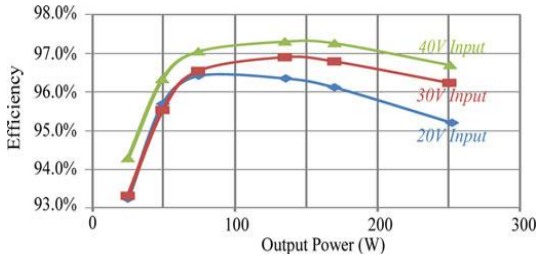

Measured power stage experimental efficiency (400-Vdc output)

4. Conclusion

As a solution for providing efficient, distributed PV conversion, an isolated boost resonant converter has been proposed. The system is a hybrid between a traditional CCM boost converter and a series-resonant half-bridge, employing only two active switches. The synthesis of the converter was described along with the circuit operating modes and key waveforms. The design process was then defined, with a focus on the unique combined resonant and PWM behavior. The result was a simple process, requiring only consideration of the resonant period length in selecting a valid converter duty cycle range. Also provided was a detailed theoretical loss analysis, along with formulas for calculating the rms values of important waveforms. Finally, the loss and theoretical analysis were verified by the design, construction, and testing of a 250-W experimental prototype. The principle advantages of utilizing this topology were as follows:

1) High weighted efficiency because of low circulating energy and reduced switching loss with resonant energy transfer and output diode ZCS;
2) Low potential cost due to minimal number of active devices and a small overall component count;
3) Galvanic isolation allows for the use of high efficiency inverter stages without additional concern over ground leakage current;
4) Reduced control complexity provides lower auxiliary power loss and simpler controller IC configurations.

Further efficiency improvements are possible with the addition of wideband gap semiconductor devices and passive component optimization.

References

[1] A. S. Masoum, F. Padovan, M. A. S. Masoum, Impact of partial shading on voltage- and current-based maximum power point tracking of solar modules, in Proc. IEEE PES General Meet., 2010, 1–5
[2] B. Brooks, C. Whitaker, Guideline for the use of the Performance Test Protocol for Evaluating Inverters Used in Grid-Connected Photovoltaic Systems [Online].Available:http://www.gosolarcalifornia.org/equipment/documents/Sandia_Guideline_2005.pdf, 2005
[3] W. Bower, C. Whitaker, W. Erdman, M. Behnke, M. Fitzgerald, Performance Test Protocol for Evaluating Inverters Used in Grid-Connected Photovoltaic Systems [Online]. Available:http://www.gosolarcalifornia.org/equipment/documents/2004-11-22_Test_Protocol.pdf, 2004
[4] O. Lopez, R. Teodorescu, F. Freijedo, J. Doval Gandoy, Leakage current evaluation of a single-phase transformer less PV inverter connected to the grid, IEEE Appl. Power Electron. Conf., 2007, 907–912
[5] W. Yu, J.-S. Lai, H. Qian, C. Hutchens, High-efficiency MOSFET inverter with H6-type configuration for photovoltaic non isolated ac-module applications, IEEE Trans. Power Electron., 26(4), 2011, 1253–1260
[6] T. Kerekes, R. Teodorescu, U. Borup, Transformer less photovoltaic inverters connected to the grid, IEEE Appl. Power Electron. Conf., 2007, 1733–1737
[7] Q. Li, P. Wolfs, Recent development in the topologies for photovoltaic module integrated converters, IEEE Power Electron. Spec. Conf., 2006, 1–8
[8] L. Gao, R. A. Dougal, S. Liu, A. P. Iotova, Parallel-connected solar PV system to address partial and rapidly fluctuating shadow conditions, IEEE Trans. Ind. Electron., 56(5), 2009, 1548–1556

[9] R. Gules, J. De Pellegrin Pacheco, H. L. Hey, J. Imhoff, A maximum power point tracking system with parallel connection for PV stand-alone applications, IEEE Trans. Ind. Electron., 55(7), 2008, 2674–2683
[10] B. Liu, S. Duan, T. Cai, Photovoltaic dc-building-module-based BIPV system: Concept and design considerations, IEEE Trans. Power Electron., 26(5), 2011, 1418–1429
[11] W. Xiao, N. Ozog, W. G. Dunford, Topology study of photovoltaic interface for maximum power point tracking, IEEE Trans. Ind. Electron., 54(3), 2007, 1696–1704
[12] L. Zhang, K. Sun,Y. Xing, L. Feng, and H. Ge, A modular grid-connected photovoltaic generation system based on dc bus, IEEE Trans. Power Electron., 26(2), 2011, 523–531
[13] Q. Li, P. Wolfs, A review of the single phase photovoltaic module integrated converter topologies with three different dc link configurations, IEEE Trans. Power Electron., 23(3), 2008, 1320–1333
[14] S. B. Kjaer, J. K. Pedersen, F. Blaabjerg, A review of single-phasegrid-connected inverters for photovoltaic modules, IEEE Trans. Ind. Appl., 41(5), 2005, 1292–1306
[15] J. M. A. Myrzik, M. Calais, String and module integrated invertersfor single-phase grid connected photovoltaic systems: A review, IEEE Bologna Power Tech Conf., 2003, 8
[16] S. B. Kjaer, J. K. Pedersen, F. Blaabjerg, Power inverter topologies for photovoltaic modules-a review, in Proc. Ind. Appl. Conf., 2002, 2, 782–788
[17] Y.-F. Huang, Y. Konishi, W.-J. Ho, Series resonant type softswitchinggrid-connected single-phase inverter employing discontinuousresonant control applied to photovoltaic ACmodule, in Proc. Appl. Power Electron. Conf., 2011, 989–994
[18] D. C. Martins, R. Demonti, Photovoltaic energy processing for utility connected system, in Proc. Ind. Electron. Soc., 2001, 2, 1292–1296
[19] E. Roman, R. Alonso, P. Ibanez, S. Elorduizapatarietxe, D. Goitia, Intelligent PV module for grid-connected PV systems, IEEE Trans. Ind. Electron., 53(4), 2006, 1066–1073
[20] Y.-C. Hsieh, M.-R.Chen, H.-L. Cheng, An interleaved flyback converterfeatured with zero-voltage transition, IEEE Trans. Power Electron., 26(1), 2011, 79–84
[21] G. Spiazzi, P. Mattavelli, A. Costabeber, High step-up ratio flybackconverter with active clamp and voltage multiplier, IEEE Trans. Power Electron., 26(11), 2011, 3205–3214
[22] M. Fornage, Method and apparatus for converting direct current to alternating current, U.S. Patent 7 796 412, 2010
[23] Y. Gu, L. Hang, Z. Lu, Z. Qian, D. Xu, Voltage doubler applicationin isolated resonant converters, in Proc. Ind. Electron. Soc., 2005, 5
[24] B. Lu, W. Liu, Y. Liang, F. C. Lee, J. D. van Wyk, Optimal design methodology for LLC resonant converter, Appl. Power Electron. Conf., 2006, 6
[25] J. F. Lazar, R. Martinelli, Steady-state analysis of the LLC seriesresonant converter, in Proc. Appl. Power Electron. Conf., 2001, 2, 728–735
[26] Z. Liang, R. Guo, J. Li, A. Q. Huang, A high-efficiency PV moduleintegrateddc/dc converter for PV energy harvest in FREEDM systems, IEEE Trans. Power Electron., 26(3), 2011, 897–909
[27] B.-G. Chung, K.-H. Yoon, S. Phum, E.-S. Kim, J.-S. Won, "A novel LLC resonant converter for wide input voltage and load range, Int. Conf. Power Electron./ECCE Asia, 2011, 2825–2830
[28] H. Hu, X. Fang, Q. Zhang, Z. J. Shen, I. Batarseh, Optimal design considerations for a modified LLC converter with wide input voltage range capability suitable for PV applications," in Proc. Energy Convers. Congr. Expo., 2011, 3096–3103
[29] A. Lohner, T. Meyer, A. Nagel, A new panel-integratable inverter concept for grid connected photovoltaic systems, IEEE Int. Symp. Ind. Electron., 1996, 2, 827–831
[30] J. Zeng, J. Ying, Q. Zhang, A novel dc/dc ZVS converter for battery input application, Appl. Power Electron. Conf., 2002, 2, 892–896
[31] K. Fathy, H. W. Lee, T. Mishima, M. Nakaokal, Boost-half bridge single power stage PWM dc-dc converter for small scale fuel cell stack, IEEE Int. Power Energy Conf., 2006, 426–431
[32] C.-E. Kim, G.-W.Moon, S.-K. Han, Voltage doubler rectified boostintegrated half bridge (VDRBHB) converter for digital car audio amplifiers, IEEE Trans. Power Electron., 22(6), 2007, 2321–2330
[33] C. Yoon, S. Choi, Multi-phase dc-dc converters using a boost halfbridge cell for high voltage and high power applications, IEEE Int. Power Electron. Motion Control Conf., 2009, 780–786
[34] S. Park, S. Choi, Soft-switched CCM boost converters with highvoltage gain for high-power applications, IEEE Trans. Power Electron., 25(5), 2010, 1211–1217
[35] N. Femia, G. Petrone, G. Spagnuolo, M. Vitelli, Optimization of perturb and observe maximum power point tracking method, IEEE Trans. Power Electron., 20(4), 2005, 963–973
[36] T. Esram, J. W. Kimball, P. T. Krein, P. L. Chapman, P. Midya, Dynamic maximum power point tracking of photovoltaic arrays usingripple correlation control, IEEE Trans. Power Electron., 21(5), 2006, 1282–1291
[37] A. F. Boehringer, Self-adapting dc converter for solar spacecraft power supply, IEEE Trans. Aerosp. Electron. Syst., AES-4(1), 1968, 102–111
[38] T. Tafticht, K. Agbossou, Development of a MPPT method for photovoltaicsystems, Can. Conf. Electr. Comput. Eng., 2004, 2, 1123–1126
[39] J. A. Gowand, C. D. Manning, Controller arrangement for boost converter systems sourced from solar photovoltaic arrays or other maximum power sources, IEE Proc.—Electr. Power Appl., 147(1), 2013, 15–20
[40] M. Veerachary, T. Senjyu, K. Uezato, Maximum power point tracking control of IDB converter supplied PV system, IEE Proc.—Electr. Power Appl., 148(6), 2001, 494–502
[41] R. W. Erickson, D. Maksimovi´c, Fundamentals of Power Electronics, 2nd ed. New York: Springer, 2001